IEEE Access
Multidisciplinary ⋮ Rapid Review ⋮ Open Access Journal

Received 12 October 2022, accepted 1 November 2022, date of publication 9 November 2022, date of current version 16 November 2022.

Digital Object Identifier 10.1109/ACCESS.2022.3220839

RESEARCH ARTICLE

Research on Spectrum Needs Prediction Method for HAPS as IMT Base Station

YUETIAN ZHOU[1,2], FEI QI[1], AND WEILIANG XIE[1]
[1]Department of Mobile Communication and Terminal Technology, China Telecom Research Institute, Beijing 100035, China
[2]National Key Laboratory of Science and Technology on Communications, University of Electronic Science and Technology of China, Chengdu 610056, China

Corresponding author: Yuetian Zhou (zhouyt@chinatelecom.cn)

This work was supported by China Telecom Corporation Ltd.

ABSTRACT The High-Altitude Platform Station (HAPS) is an integral component in Non-Terrestrial Network (NTN) which is potential 6G technology. The HAPS as IMT Base Stations (HIBS) in the mobile service is an emerging and promising approach to achieve vertical heterogeneous network. Therefore, some efforts have been made in order to harmonize the worldwide usage of HIBS, including investigations of the spectrum needs, usage, and technical and operational characteristics of HIBS, among which the spectrum needs has drawn particular attention because it should be determined in advance prior to the commercial deployment of HIBS. However, there are very few investigations devoted to the prediction of the spectrum needs for future HIBS deployments currently due to some tough difficulties. Firstly, there has no actual deployment precedent of HIBS so that the future capacity demands are not clear. Secondly, both the networking and its performance of HIBS deployment are questions to be answered. Therefore, taking into account the study under WRC-23 Agenda Item 1.4 HIBS-CHARACTERISTICS, this paper proposes an evaluation method of the spectrum needs prediction for HIBS deployed as a supplementary for grounded base station, and presents the results of spectrum needs for HIBS in certain frequency bands identified for IMT. The capacity demand of HIBS in 2025 is predicted and the spectral efficiency of HIBS system is obtained by simulation, and the spectrum needs is defined as *Capacity Demand/Spectral Efficiency*. The main contributions of this paper are as follows: Firstly, to obtain the spectral efficiency of HIBS systems, we set up a simulation model with 7-cell networking in accordance with configuration parameters of WRC-23 AI 1.4, which equipped with beamforming antenna to improve spectral efficiency. And calculating the CDF curve of spectral efficiency by using Monte Carlo method allows the simulation result to more closely match the actual deployment. Secondly, in order to solve the problem of no actual HIBS traffic data, we propose a method based on the methodology provided in Recommendation ITU-R M.1768-1 to simulate the capacity demand, and then to predict the capacity demand of HIBS in 2025 by polynomial fitting. Finally, we have predicted the spectrum needs by calculating *Capacity Demand/Spectral Efficiency.* The spectrum demand range of HIBS for China rural area in 2025 predicted by the proposed method is from 80.30 MHz to 122.97 MHz. This method can effectively predict the spectrum needs of HIBS for various deployment scenarios, which plays an important role in driving the commercial deployment of HIBS.

INDEX TERMS 6G, HIBS\HAPS, NTN, beamforming antenna, traffic prediction, 7-cell networking.

I. INTRODUCTION

Aim to realize the vision of 6G three-layer vertical heterogeneous network, the NTN is one of the promising 6G technology discussed widely, which is defined in 3GPP Technical Report 38.811 [1]. The important components of NTN include satellite system, HAPS and UAV etc. Since HAPS have larger coverage and capacity than UAV, as well as satellite system experience high path loss and higher delay than HAPS [2], [3], the use of HAPS as IMT base station

The associate editor coordinating the review of this manuscript and approving it for publication was Bilal Khawaja.

This work is licensed under a Creative Commons Attribution 4.0 License. For more information, see https://creativecommons.org/licenses/by/4.0/

is an emerging and significant method to enhance mobile network.

The HAPS is a network node that operates at the altitude of 20-50 km above the ground, and can stay at quasi-stationary [4]. HAPS related work can be traced back to 1990s [5], which is showed promise for the advantage of coverage and deployment convenience, with a particularly on emergency relief and remote areas. However, because of the limitation of aircraft load capacity as well as energy, HAPS has not been commercially available so far. Due to the development of the technology of battery, solar panel [6], [7], lightweight materials and autonomous avionics in the last decade [8], HIBS\HAPS is widely considered become more economically feasible in the 6G era. The commercial and research project deployments instance of HAPS systems was introduced in [9], and a summary of past field trials and experimental studies along with open technical issues as well as current application was given in [10] and [11]. And some literatures have discussed the role of HAPS in vertical NTN. The use of HAPS as either a stand-alone or complementary of the terrestrial network was discussed in books [12], [13]. Reference [14] demonstrated the integration of the satellite systems and HAPS, bridging the wide gap between the terrestrial and satellite communication systems. Moreover, the basic issues for HAPS should regain attention. The channel models for HAPS of SISO and MIMO were demonstrated in [15], and propagation modeling was discussed in [16], [17], and [18]. And in recent years, some fresh views and research on the applications and technologies of HAPS are given in [19] and [20]. The promising research directions about communication and computation of HAPS in the next generation are introduced in [19], such as HAPS mounted Super Macro Base Station (SMBS), use of Reconfigurable Intelligent Surface (RIS) in the communications payload of HAPS, Radio Resource Management (RRM) and interference management of HAPS, AI and Machine Learning (ML) in HAPS and so on. And the [20] positions HAPS in the era of 6G by various applications for large scale communications, computation offloading, intelligent relaying, and distributed ML.

Although HAPS is one of the most promising 6G technology, harmonizing the worldwide usage have to pay more attention to regulations of aviation and spectrum. The regulation activities are limited by the ITU-R and International Civil Aviation Organization (ICAO). ITU-R regulates spectrum aspects related to HAPS while ICAO governs the aviation safety and activities of HAPS [21]. ICAO defines two distinct classes of HAPS, one is unmanned free balloons and the other is the unmanned aircraft. The difference between the two is that balloons are excluded from real-time management [22]. Regulatory guidance is still developing, which will affect local market choices [22]. As for spectrum aspects, the World Radiocommunication Conference in 2019 (WRC-19) has revised the spectrum regulatory framework for HAPS. The allocations dedicated for HAPS can be found in [23], [24], and [25]. ITU-R provides flexibility of spectrum usage for HAPS while ensuring protection of the existing services, therefore a large number of sharing and compatibility studies have been carried out [23], [24], [25].

HAPS has great potential in various application of the next generation, however promoting HAPS as IMT base stations (HIBS) in the mobile service is the first thing to be done. Current technologies could enable HIBS to provide low latency and broadband mobile connectivity in rural, remote area and underserved area, over a large geographic footprint, as well as using the same frequency to support and complement the IMT-grounded network in urban. Therefore, WRC-19 adopted Resolution 247 (WRC-19) and has resolved to identify Agenda Item 1.4 of WRC-23: *Study the use of high-altitude platform stations as IMT base stations (HIBS) in the mobile service in certain frequency bands below 2.7 GHz already identified for IMT* [26].

Determining spectrum needs are a precondition for commercial deployment. The spectrum needs dependent on a number of factors, such as specific system characteristics and deployment scenarios. Based on WRC23 Agenda Item 1.4, while taking into account sharing and compatibility with existing service, this paper outlines technical and operational characteristics, as well as corresponding usage and deployment scenarios for HIBS in mobile service in certain bands below 2.7 GHz already identified for IMT, and then proposes an evaluation method to predict the spectrum needs of HIBS in specific deployment scenario in 2025 years. The paper is organized as follows: Section II descripts the system model of HIBS, including the system architecture, network topology and antenna model, and gives the simulation parameters; Section III presents an algorithm to simulate the HIBS's spectral efficiency based on Monte Carlo system simulation; Section IV gives a method to predict the capacity demand of HIBS in 2025, as well as the calculate result of spectrum needs. A conclusion is given in Section V.

II. SYSTEM MODEL AND CONFIGURATION

Since the application scenarios determine the characteristics of the communication system used, spectrum needs are affected by the specific usage and deployment scenario. The technical characteristics given in this section are aimed at case that HIBS is deployed to complement for the grounded IMT networks in unserved areas, extending the coverage, providing connectivity and applications including emergency responses, disaster relief and sensor networks.

A. SYSTEM ARCHITECTURE

Figure 1 shows a system architecture diagram of HIBS used in this paper's deployment scenario. The HAPS equips 7 Active Antenna Units (AAU) to provide 7 service cells, and the service link and gateway link make up the HIBS network.

Service link communicates between HIBS and user equipment (UE) utilizing frequency which is already identified for IMT. Since UE has the low transmit power and the omni-directional antenna (which gain is low), HIBS require high gain antenna to transmit and receive signals

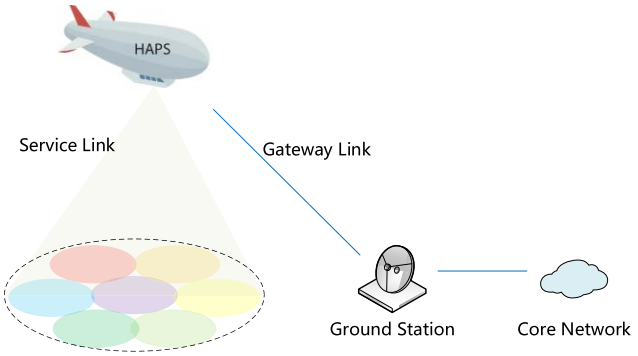

FIGURE 1. HIBS system architecture diagram.

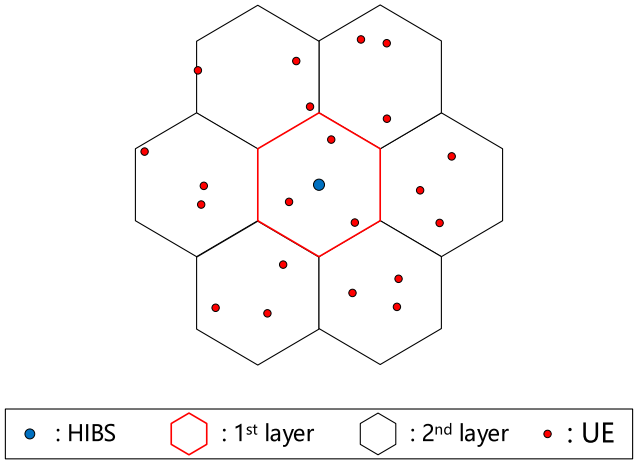

FIGURE 2. 7 cells deployment diagram.

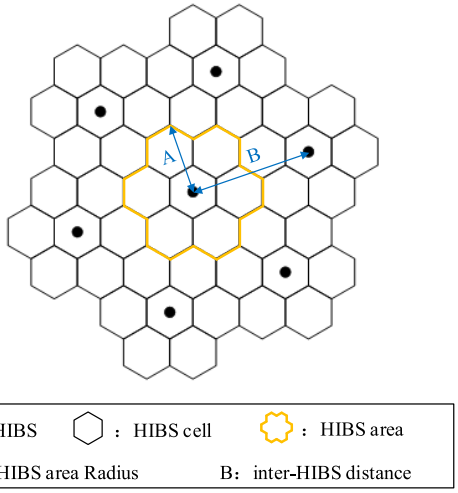

FIGURE 3. A cluster of HIBS networking topology.

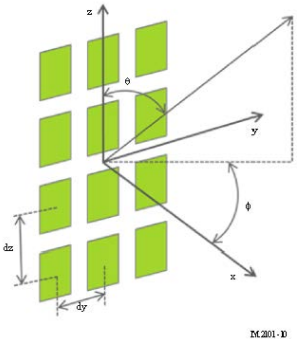

FIGURE 4. Antenna model geometry.

appropriately. Thus, the MIMO antenna is equipped to provide connectivity over a wide area. Moreover, beamforming and mechanical tilt will be adopted to overcome the unstable of air-carrier, which is implemented to ensure stable connectivity.

Gateway link provides a backhaul connection between the HIBS and core network via the dedicated ground station.

B. NETWORK TOPOLOGY

Since HAPS equipped 7 AAUs in the deployment scenario of this paper, a HIBS area can be divided into 7 cells with multi-beam configurations as shown in the Figure 2. The cell at the center of the HIBS area is 1st layer cell, and the cells on the outside arranged at equal horizontal angle interval (60 degree) are defined as 2nd layer cell. The reason why HIBS has such a cell topology is because of the arrangement of AAUs on the HAPS, related parameters are illustrated in section II.D.

The networking topology for a cluster of HIBS deployed in wider area is shown in Figure 3. There are 7 HIBS areas and each area covered by single HIBS. *HIBS area Radius* is defined as A while distance between HIBS referred to *inter-HIBS distance* is defined as B. Moreover, B can be calculated by A as $B = \sqrt{3}\,A$. The system simulation of this paper is utilizing the topology structure of Figure 3.

C. ANTENNA MODEL

The antenna (AAU) equipped on the HAPS has the ability of beamforming, which should be consider in this simulation. The muti-beam scheme will affect the calculation of signal and interference. As shown in Figure 4, the beamforming antenna is based on an antenna array and consists of a number of identical radiating elements located in the same plane with a fixed separation distance. The radiation patterns of all elements pointing along the x-axis, and system using an AAU will actively control all individual signals being fed to individual antenna elements in the antenna array aim to shape and direct the antenna pattern to a wanted shape.

The radiation elements of antenna model illustrated in the Figure 4 are placed uniformly on the z-O-y vertical plane in the cartesian coordinate system. The x-O-y plane denotes the horizontal plane. The elevation angle of the signal direction is denoted as θ which defined between 0° and 180°, with 90° representing perpendicular angle to the array antenna aperture. The azimuth angle is denoted as Φ which defined between $-180°$ and 180°.

The antenna array model is determined by element pattern, array factor and signals applied to the array system. The

single element pattern is calculated by (1)-(3) [27]:

$$A_{E,H}(\phi) = -\min\left[12\left(\frac{\phi}{\phi_{3dB}}\right)^2, A_m\right] \quad (1)$$

$$A_{E,V}(\theta) = -\min\left[12\left(\frac{\theta-90}{\theta_{3dB}}\right)^2, SLA_v\right] \quad (2)$$

$$A_E(\phi,\theta) = G_{E,max} - min\left\{-\left[A_{E,H}(\phi) + A_{E,v}(\theta)\right], A_m\right\} \quad (3)$$

The horizontal and vertical radiation pattern of element is calculated by (1) and (2) respectively, where ϕ_{3dB} and θ_{3dB} are 3dB bandwidth of horizontal and vertical, A_m and SLA_v are the front-to-back ratio. The element pattern calculated by (3) is the vector sum of $A_{E,H}(\phi)$ and $A_{E,V}(\theta)$, where $G_{E,max}$ is element gain. The (4) derived by (3) illustrates composite antenna beamforming pattern, which is the sum of element gain and array gain:

$$A_{A,Beami}(\theta,\phi) = A_E(\theta,\phi) + 10log_{10}\left(\left|\sum_{m=1}^{N_H}\sum_{n=1}^{N_V} w_{i,n,m}\cdot v_{n,m}\right|^2\right) \quad (4)$$

The second item in (4) is logarithmic sum of the array gain, where $w_{i,n,m}$ is a weighting function used to direct the beam in various directions, and $v_{n,m}$ is the super position vector. These two factors are related to θ, φ and element spacing, the specific calculation is given in [27]. N_H and N_V is the number of elements along the horizontal and vertical respectively. The composite pattern should be used where the array serves one or more UEs with one or more beams, with each beam indicated by the parameter i.

D. CONFIGURATION PARAMETERS

This paper will carry out system simulation on 3 frequency bands, which are the largest service volume of Chinese operators at present. The Table 1[Note2] demonstrates the deployment related configuration parameters of HIBS and the UE served by HIBS.

TABLE 1. Deployment related parameters of HIBS and the UE served by HIBS in simulation.

Parameter	Band 1 (694-960 MHz)	Band 2 (1710-1980/2010-2025/2110-2170MHz)	Band 3 (2500-2690 MHz)
HIBS characteristics			
HIBS area radius	100 km	100 km	90 km
HIBS Altitude	20km		
Operate bandwidth	20MHz		
Frequency reuse	1		
Element gain	8 dBi		
Horizontal/vertical 3 dB beamwidth of single element	65º for both H/V		
Horizontal/vertical front-to-back ratio	30 dB for both H/V		
Antenna array configuration (Row × Column)	2 x 2 elements (1st layer cell), 4 x 2 elements per cell (2nd layer cell)		
Horizontal/Vertical radiating element spacing	0.5 of wavelength for both H/V		
Ohmic losses	2 dB		
HIBS Platform Antenna tilt	90º (1st layer cell), 33º (2nd layer cell)	90º (1st layer cell), 23º (2nd layer cell)	90º (1st layer cell), 23º (2nd layer cell)
HIBS Conducted power per antenna element	37 dBm (1st layer cell), 34 dBm (2nd layer cell)		
HIBS Platform e.i.r.p./cell	55 dBm (1st layer cell), 58 dBm (2nd layer cell)		
UE characteristics			
UE density	3 UEs per cell		
UE height	1.5 m		
Body loss	4 dB		
Antenna gain	-3 dBi		
Maximum transmitter power	23 dBm		

III. SIMULATION OF SPECTRAL EFFICIENCY

In this section, we use Monte Carlo experimental method to perform system level simulation to calculate spectral efficiency. We randomly distribute users in the network topology shown in Figure 3 and calculate the spectral efficiency of each user point, which process is called a ''snapshot''. After taking multiple snapshots, we will obtain the spectral efficiency of a large number of points, which covers almost all positions in the topological network. The average value can be regarded as the spectral efficiency of the system.

A. USER ACCESS METHOD

Firstly, it is necessary to consider which cell the UE accesses. The UE is distributed in HIBS area randomly, we assume the user density is 3 UEs/cell (shown in Table 1). The Figure 2 is an instance for the users' distribution of a snapshot, and the Figure 3 is the networking topology in the simulation (7 HIBS areas, and 7 cells/HIBS). The flowchart of access process for a single HIBS is illustrated in Figure 5.

The specific creation methodology of the access process in the simulation is as follows:

Step 1: UE is randomly deployed in a circle with the $HIBS_i$ ($i \in [1, 7]$) as the centre and the HIBS area radius as the radius.

Step 2: for each UE, calculating the transmit power P_{tx}, the antenna gain G_{tx} and the total $Loss$ (includes propagation loss, ohmic loss, body loss and penetration loss, etc.) from each HIBS cell, and calculating the

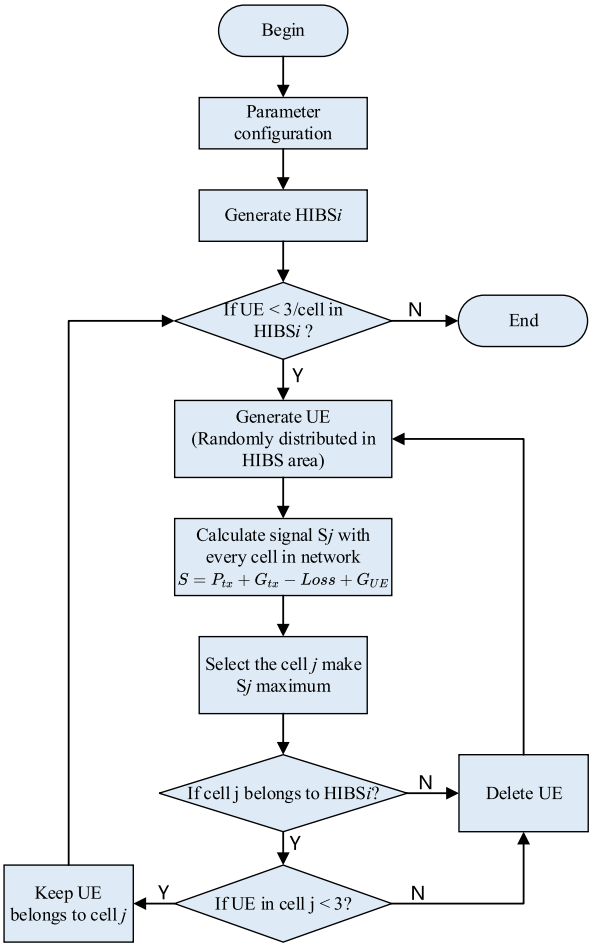

FIGURE 5. Flowchart of UE access process.

signal S from $cell_j$ ($j \in [1, 49]$) by (5)[Note1]:

$$S_j = P_{tx,j} + G_{tx,j} - Loss_j + G_{UE} \tag{5}$$

Step 3: selecting the HIBS $cell_j$ to make the S maximum.
Step 4: if the $cell_j$ belongs to the $HIBS_i$, execute the Step 5; Otherwise, delete the UE and regenerate UE to repeat the Step 1 to Step 4.
Step 5: if the number of UE in $cell_j < 3$, keep UE belongs to $cell_j$; Otherwise, delete the UE and regenerate UE to repeat the Step 1 to Step 4.
Step 6: iterate the $HIBS_i$ from $i = 1$ to 7.

The algorithm complexity of UE access is O(nj^2), where n is the number of snapshots and j is the number of cells.

Note 1: S_j is calculated by 4 items in (5). G_{UE} is fixed, and $P_{tx,j}$ has two + values which is depended on whether it is power of 1st layer cell or 2nd layer cell, the parameters of two items can be find in Table 1. $Loss_j$ is calculated by propagation loss $ProL$ and other loss (includes ohmic loss, body loss and penetration loss. Other loss is fixed in the simulation, and pathloss adopt propagation model by (6) [28], where r is the distance between the base station on HAPS and UE.

TABLE 2. Parameters describing link level performance for HIBS.

Parameter	DL	UL
α	0.6	0.4
$SINR_{min}$ (dB)	−10	−10
$SINR_{max}$ (dB)	30	22

$$ProL = 20log_{10}f + 20log_{10}r + 32.44(dB) \tag{6}$$

As for $G_{tx,j}$, the antenna model use the model in Section II.C, the maximum gain direction of antenna is pointing the centre of each cell. The $G_{tx,j}$ is depending on the θ and φ of the antenna which are determined by coordinates of centre of $cell_j$, UE and $HIBS_i$.

B. DOWNLINK SPECTRAL EFFICIENCY

In order to calculate the spectral efficiency of a randomly distributed UE, it is necessary to calculate the SINR of the UE. For downlink, the UE in the topology network of the simulation will receive signals from antenna of 49 cells (7×7, 7 HIBS areas and 7 cells/HIBS), denoted as S_j ($j \in [1, 49]$). Assume that, while $j = k$, signal has the maximum value $S_{max} = S_k$, which means that the UE accesses $cell_k$ and S_k is the wanted signal. Thus, $\{S_j \,|\, j \in [1, 49] \cap j \neq k\}$ is the interference signal, denote $S_j as I_j (j \neq k)$. I_j represents that UE receive the interference of $cell_j$, therefore the aggregate interference I_{sum} is calculated by (7), and SINR of the UE is calculated by (8), which unit is dB.

$$I_{sum} = 10log_{10}\left(\sum_{j=1,j\neq k}^{49} 10^{\frac{I_j}{10}}\right) \tag{7}$$

$$SINR_{downlink} = S_k - 10log_{10}\left(10^{\frac{I_{sum}}{10}} + 10^{\frac{N}{10}}\right) \tag{8}$$

The N is the noise, it depends on thermal noise of UE for downlink, and takes the typical value of $-105dB$ in the simulation. According to the SINR, the spectral efficiency f_{se} of the UE at that coordinate point under the HIBS deployed in this paper can be calculated by (9), which is derived by Shannon bound.

$$f_{se}(\text{inbps/HZ}) = \begin{cases} 0 & SINR < SINR_{min} \\ \alpha \cdot log_2(1 + SINR) & SINR_{min} \leq SINR < SINR_{max} \\ \alpha \cdot log_2(1 + SINR_{max}) & SINR \geq SINR_{max} \end{cases} \tag{9}$$

The α is attenuation factor, representing implementation losses. $SINR_{min}$ and $SINR_{max}$ are the boundary of SINR of the code set. The parameters α, $SINR_{min}$ and $SINR_{max}$ can be chosen to represent different modem implementations and link conditions, which are demonstrated in Table 2[Note2] for implementation of this paper.

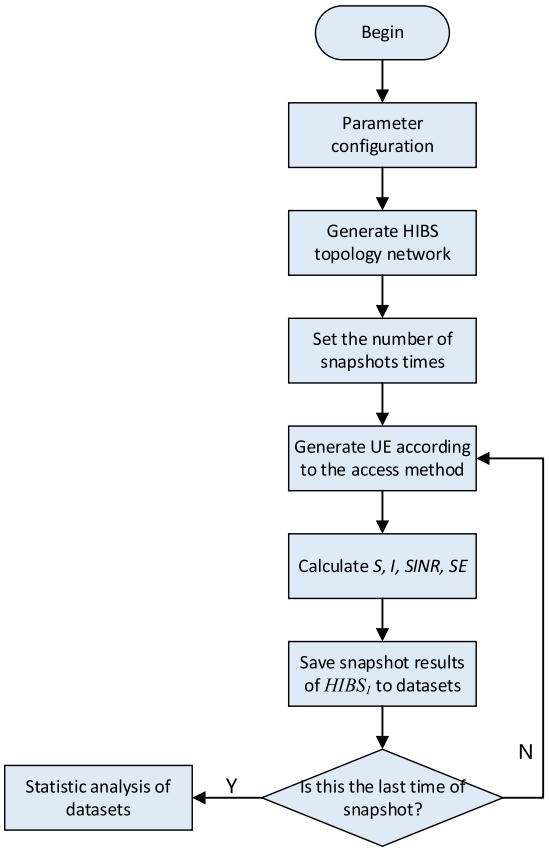

FIGURE 6. Flowchart of downlink spectral efficiency method.

Note 2: The parameters in Table 1 and Table 2 are the parameters determined in the ITU-R AI 1.4 PDNR (Preliminary Draft New Report) after discussion by delegates of each country. The other contents in the PDNR need to be updated in several meetings for discussion before the official ITU report can be formed for the public. Therefore, there is no specific public reference for these parameters.

Through (7), (8) and (9) we can obtain spectral efficiency of one point in the HIBS coverage, using this calculation multiple times can obtain the spectral efficiency of all points in a snapshot. By taking multiple snapshots, we can get the uniform distribution of UE in HIBS coverage and a large number of spectral efficiency datasets of coordinate points corresponding to UEs. The flowchart of downlink simulation method is illustrated as Figure 6.

The algorithm complexity of DL calculation is O(nj^2), where n is the number of snapshots and j is the number of cells. The specific steps will not be repeated here, however there are several points to be explained. The $HIBS_1$ in Figure 6 is the center of the topology network shown in the Figure 3. Since it is a typical networking situation that $HIBS_1$ is interfered by surrounding HIBS, we only investigate the spectral efficiency point distribution of $HIBS_1$. The dataset saves the SE, SINR, S, and I of points belonging to $HIBS_1$ in all snapshots, and statistical analysis of the dataset will reveal the results of downlink spectral efficiency.

C. UPLINK SPECTRAL EFFICIENCY

Since SE of uplink is constrained by interference from other UEs, power control is necessary considered, which can be combined with frequency-domain resource allocation strategies to enhance cell edge performance as well as improve SE [27]. The algorithm of power control for single UE is as (10), (11), (12), where P_a is the power of UE for allocating the maximum resource block (RB) $M_{\max}$, P_{0pusch} is power per RB, α is balancing factor for UEs with bad channel and good channel; $PathL$ is pathloss including propagation loss, body loss, ohmic loss, and gain of HIBS and UE, G_{HIBS} is determined by the antenna model illustrated in section II; P_{UE} is the UE's power, P_{cmax} is the maximum power of UE.

$$P_a = 10log_{10}(M_{\max}) + P_{0pusch} + \alpha \cdot PathL \quad (10)$$

$$PathL = ProL + BodyL + omL - G_{HIBS} - G_{UE} \quad (11)$$

$$P_{UE} = min(P_a, P_{cmax}) \quad (12)$$

And the number of allocated RB M_{UE} of the power control is:

$$M_{UE} = \begin{cases} M_{max} & (P_a < P_{cmax}) \\ 10^{\frac{P_{UE} - \alpha \cdot PathL - P_{0pusch}}{10}} & (P_a \geq P_{cmax}) \end{cases} \quad (13)$$

The related parameters of power control in the simulation are as follows: $M_{\max}$ is 105 RB, P_{0pusch} is -92.2 dBm, α is 0.8. Others can be found in Table 1.

However, the UEs in the same cell need to cooperative schedule, the M_{UE} should modify according to the other 2 UE in the same cell. Therefore, the actual used RB of the UE is:

$$M_{actual} = \frac{M_{UE}}{M_{UE} + M_{UEp} + M_{UEq}} \times M_{max} \quad (14)$$

The M_{UEp} and M_{UEq} is the allocated RB calculated by (13) of the other 2 UE in the same cell. So far, we have completed the resource allocation and power calculation of a single UE under the power control algorithm. It is worth noting that the different UE have the different power spectral density, so it's better to calculate S, I, SINR for uplink by using power per MHz. Thus, the uplink signal power density of the jth user served in the ith cell ($UE_{i,j}$) denoted as $P_{i,j}$ is (15), $i \in [1, 49], j \in [1, 3]$:

$$P_{i,j} = P_{UE}^{i,j} - 10log_{10}\left(M_{actual}^{i,j} \times \frac{180}{1000}\right) \quad (15)$$

Then, we can calculate the S, I, and SINR for uplink. The signal strength $S_{i,j}^k$ is defined as the transmit signal power of the $UE_{i,j}$ received at BS antenna of $cell_k$. While $k = i$, the $S_{i,j}^i$ is the useful signal. And the other UEs, which are served in different cell, their transmit power received at BS antenna of $cell_i$ are defined as the interference, that is, $\left\{S_{x,y}^i \,|\, x \neq i, x \in [1, 49], y \in [1, 3]\right\}$ are the interference signal, denote interference as $I_{x,y}^i$; The other two UEs, which are served in same cell, that is, $\left\{UE_{i,y} \,|\, y \neq j, y \in [1, 3]\right\}$ are cooperative schedule with $UE_{i,j}$, so their transmit power is not interference. Hence, for the $UE_{i,j}$, useful signal $S_{i,j}^i$, the interference $I_{x,y}^i$ and aggregate interference I_{sum}^i for uplink,

and the uplink SINR can be calculated via (16), (17), (18), (19) [Note3]:

$$S^i_{i,j} = P_{i,j} + G^i_{i,j} - Loss^i_{i,j} + G_{UE} \tag{16}$$

$$I^i_{x,y} = S^i_{x,y} + 10log_{10}\left(\frac{M^{x,y}_{actual}}{M_{max}}\right)(x \neq i) \tag{17}$$

$$I^i_{sum} = 10log_{10}\left(\sum_{x=1,x\neq i}^{49}\sum_{y=1}^{3} 10^{\frac{I^i_{x,y}}{10}}\right) \tag{18}$$

$$SINR_{uplink} = S^i_{i,j} - 10log_{10}\left(10^{\frac{I^i_{sum}}{10}} + 10^{\frac{N}{10}}\right) \tag{19}$$

Note 3: There are some explanations and analysis for (16)-(19). The (16) is similar as (5) for downlink, the transmit power is replaced by the power density of $UE_{i,j}$; $G^i_{i,j}$ is the gain of antenna of $cell_i$ which is calculated by antenna model; $Loss^i_{i,j}$ is the loss from the coordinate point of $UE_{i,j}$ to $cell_i$, which includes ohmic loss, body loss, penetration loss, and propagation calculated by (6). The (17) describe interference at received antenna of $cell_i$ from the other UEs served in different cell with $UE_{i,j}$ to $cell_i$; The second item in (17) is a weighting factor, in order to obtain the average interference of different UEs in the same neighbor-cell over the total bandwidth. The (18) is the calculation of aggregate interference, which is the sum of the signal from 144 UEs except the 3 UEs in the $cell_i$. The (19) describe the uplink SINR of the $UE_{i,j}$, the N is the noise, it depends on thermal noise of HIBS which takes the typical value of $-109dB$.

Substituting the uplink SINR into (9), we can get the uplink SE of the $UE_{i,j}$ at that point. Calculating all UEs in a snapshot, and taking hundreds of snapshots, the SE of a dataset uniformly distributed in the topology network is obtained. The flowchart of uplink simulation method is similar with Figure 6, compared with the downlink, only in the snapshot cycle, the UE adds a step of ''power control method'' after completing the access process, which is not repeated here. The algorithm complexity of UL calculation is O(nj^2), which is same to DL.

D. SIMULATION RESULTS

We utilize the above method to simulate 3 frequency bands (shown in Table 1) below 2.7 GHz which is already identified for IMT. With analyzing the datasets obtained by above method, some simulation results are demonstrated in this section.

The simulation result configured snapshot=100 of access process in Band 1 and Band 3 is shown in Fig. 7, which reveals the coverage of each cell. The spots (2100 in total) of different color represent UE served in different cell. Because of 7 cells topology structure, platform antenna tilt and beamforming antenna pattern, the coverage of center cell shrinks. In the simulation process, we also found that, under this HIBS configuration, the lower the frequency band, the smaller the coverage of the central cell. Taking Band1 and band3 as an example, we can observe that the red coverage of the low frequency Band 1 is smaller.

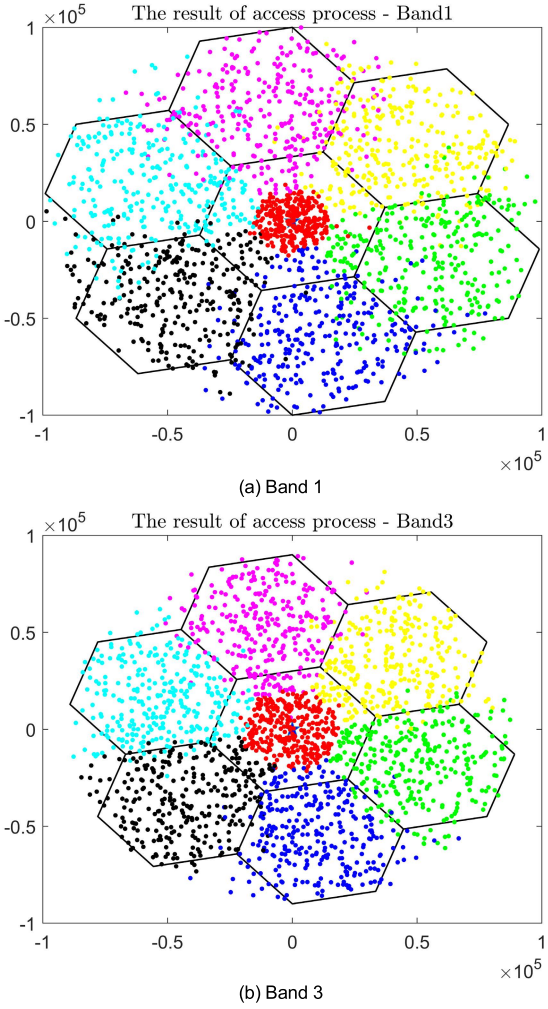

FIGURE 7. UE distribution of each cell after access process.

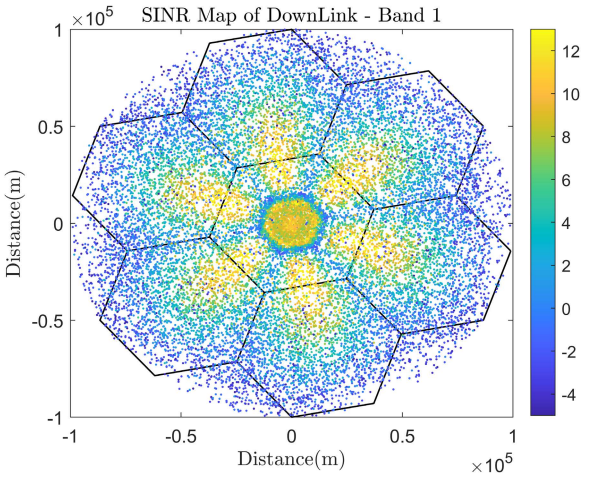

FIGURE 8. The SINR Map of downlink for Band 1.

Although the coverage of the central area is shrunk, the central area has very good signal quality. We configured snapshots=1000 and carried simulation, taking SINR map of

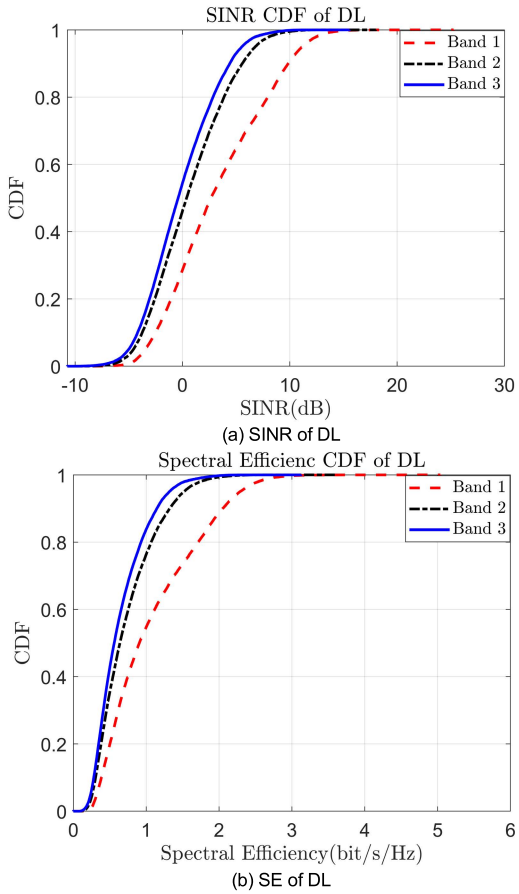

FIGURE 9. CDF curves of simulation results for downlink.

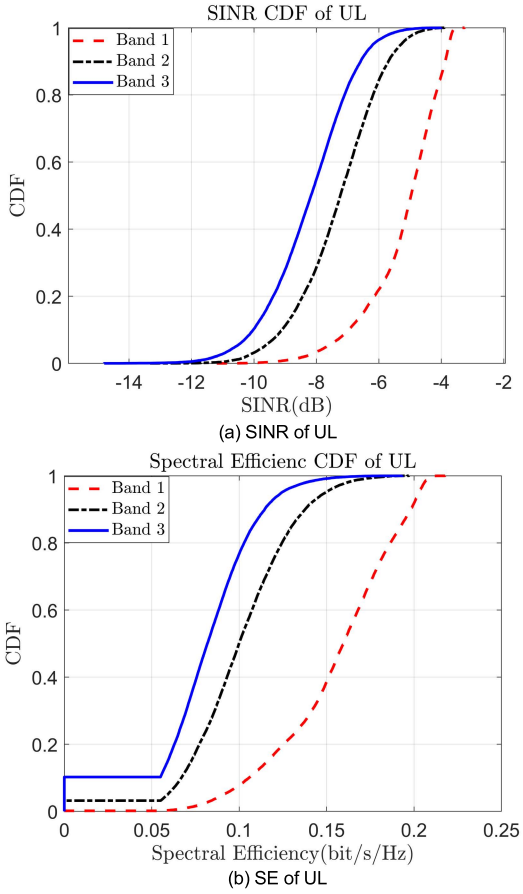

FIGURE 10. CDF curves of simulation results for downlink.

downlink for Band 1 as an example, as shown in Fig. 8, the SINR of the central cell is basically higher than 10dB, while the hot spots of the surrounding 6 cells are radially extending outward from the central cell. Hot spots throughout the HIBS area are shaped like a flower.

Then we do statistical analysis on the dataset of the simulation results (snapshots=1000). Here CDF curves are made for SINR and SE of downlink and uplink respectively, which are illustrated in Fig. 9 and Fig. 10.

According to FIG. 9 and FIG. 10, we can find that the band with lower frequency has better signal quality and spectral efficiency in the simulation under the same configuration. However, in the actual situation, the antenna size in the low-frequency band is larger, which requires higher carrying capacity of the aircraft, and the poor beam forming ability of the low-frequency band antenna needs to be overcome.

We use the 5th percentile of the CDF curve to represent the communication capability of the edge coverage of the HIBS system. As shown in Fig. 10 (b), the 5th percentile of the CDF curve of the uplink SE for Band 3 is 0 bps/Hz, which indicates that the UE is limited in uplink at the edge of HIBS and cannot access the base station equipped on HAPS. Therefore, in planning, the coverage radius of HIBS area under Band 3 should be appropriately reduced, or the capability of the airborne base station should be improved to solve this problem.

TABLE 3. Simulation result of average SINR and SE.

		Band 1	Band 2	Band 3
DL	SINR	5.83 dB	2.19 dB	1.22 dB
	SE	1.09 bit/s/Hz	0.74 bit/s/Hz	0.65 bit/s/Hz
UL	SINR	-5.07 dB	-7.13 dB	-8.05 dB
	SE	0.16 bit/s/Hz	0.1 bit/s/Hz	0.08 bit/s/Hz

We use the average value of the dataset (snapshots=1000, UE=21000) to represent the communication capability of the HIBS system, and calculate the average SINR and SE respectively for subsequent calculation of spectrum needs. The calculation results of uplink and downlink in three frequency bands are shown in Table 3.

IV. CAPACITY DEMAND AND SPECTRUM NEEDS

When deployed as complement for existing ground-based IMT network, the capacity demands of HIBS are similar to those of terrestrial IMT, which were already identified in Report ITU-R M.2290 [29] on future capacity demands

TABLE 4. The identification of service categories.

Service type \ Traffic class	Conversational	Streaming	Interactive	Background
Super-high multimedia	SC1	SC6	SC11	SC16
High multimedia	SC2	SC7	SC12	SC17
Medium multimedia	SC3	SC8	SC13	SC18
Low-rate data and low multimedia	SC4	SC9	SC14	SC19
Very low-rate data	SC5	SC10	SC15	SC20

TABLE 5. The identification of service environments.

Service usage pattern \ Tele density	Dense urban	Suburban	Rural
Home	SE1	SE4	SE6
Office	SE2	SE5	
Public area	SE3		

TABLE 6. Percentage value of market attributes settings.

Year	SC	U (%)	Q (%)	R (%)	μ (%)
2010	15	0	30	0	30
	20	0	30	0	30
2015	15	0.1	30	0	30
	20	0.1	30	0	30
2020	15	0.1	30	0	30
	20	0.1	30	0	30

estimate for terrestrial IMT. In the case of this paper, HIBS is deployed in remote areas, where ground-based IMT base stations are yet to be deployed, HIBS would play the essential role to bridge the digital divide across the rural and remote areas. In this section, we predict the spectrum needs in 2025 year for this case of HIBS application.

A. ESTIMATE METHODOLOGY

We refer the method in Report ITU-R M.2290 to estimate capacity demand of HIBS, and combine the simulation result of spectral efficiency to predict the spectrum needs in 2025. The specific methodology flow for spectrum needs is as follows:

Step 1: Refer to Recommendation ITU-R M.1768 [30] and definite the service environments (SEs) and service categories (SCs).

Step 2: According to the characteristics of the HIBS applications, select the appropriate SCs and SEs in the market data. The Spectrum requirement estimation tool for IMT [31] provides the calculation of market data for 2010, 2015 and 2020.

Step 3: Calculate the traffic demand for the selected SCs and SEs, that is, the traffic demand for the application of HIBS. The calculation method refers to the 3.5.2.6 of reference [30].

Step 4: The spectrum needs is calculated by the *CapacityDemand*/*SpectrumEfficiency*.

Step 5: Fit the existing market data through different extrapolation functions such as polynomial or exponential function, and calculate the range of traffic demand in 2025 based on the fitting curve.

The SCs are defined as the combinations of service type and traffic class, while SEs are defined for the combinations of tele density and service usage patterns. They are shown in the Table 4 and Table 5 respectively.

Since HIBS in this paper's case is deployed in remote areas, where are vast territories with a sparse population, as complement for ground-based IMT network, the user density is very low as well as the data rate of requirement. Therefore, it is suitable to choose SC15 and SC20 of SE6 as traffic estimates for the HIBS deployed scenarios, that is, (SC15, SE6) and (SC20, SE6) are the appropriate selection in the Step 2 of method flow. The capacity demand for HIBS is the sum of the traffic of (SC15, SE6) and (SC15, SE6).

B. INPUT PARAMETER CONFIG

Market related input parameters includes user density, session arrival rate per user, average session duration, mean service bit rate, which are used in the calculation of the capacity demand mentioned in Step 3.

The unique values for the market parameters selected from the ranges (maximum and minimum) given in [31] are determined through percentage values (0-100). Percentage value 0 means the minimum value inside the range and 100 means the maximum value inside the range. Table 6 is the corresponding market attributes of percentage value of the HIBS application for remote areas of China in 2010, 2015 and 2020. The capacity calculation for packet switched SCs is done as a multiplication of user density (U), session arrival rate per user (Q), mean service bit rate (R), and average session duration (μ). The numerical value of capacity is calculated as the multiplication of foregoing four market parameters. If all are changed at the same time, the resulting traffic calculation may become unnecessarily complicated. Therefore, the user density is the only market setting parameter that differs in the different setting.

The numerical values of market attributes used in the capacity demand calculation can be calculated as follow, e.g.:

$$U = x\% \cdot Maximum + (1 - x\%) \cdot Minimum \qquad (20)$$

where x is the percentage in Table 6, and Q, R, μ are the same. The maximum and minimum of market attributes settings can be looked up in [31]. The three years capacity estimates are

TABLE 7. Percentage value of market attributes settings.

Year	SC	SE	U (users/km^2)	Q (sessions/h/users)	R (kbit/s)	μ (s)	Traffic (kbit/h/km^2)	Total (kbit/h/km^2)	bps/km^2
2020	15	6	12.77	2.6523	16	30.7	16638.18	18282.18	5078.38
	20	6	10	0.411	16	25	1644		
2015	15	6	12.70	1.7221	16	15.6	5458.06	5840.14	1622.26
	20	6	10	0.199	16	12	382.08		
2010	15	6	10	1.2664	16	9.2	1864.14	1960.14	544.48
	20	6	10	0.1	16	6	96		

TABLE 8. Capacity demand of HIBS downlink.

Downlink	Band1	Band2	Band3
HIBS area radius (KM)	100	100	90
Area/HIBS cell (KM^2)	4330.13	4330.13	3507.40
2010 Traffic/cell (Mbps)	2.36	2.36	1.91
2015 Traffic/cell (Mbps)	7.02	7.02	5.69
2020 Traffic/cell (Mbps)	21.99	21.99	17.81
2025 Traffic Prediction/cell (Mbps)	47.27	47.27	38.27

calculated according to the Table 6 and (20), which is illustrated in Table 7. In addition, the calculated results of Table 7 represents the estimation of downlink capacity demand per km^2 area for the HIBS.

C. CALCULATION RESULT

Since the 7 cells of HIBS multiplex frequencies, we only need to calculate the spectrum needs through the capacity demand of one cell, that is, the spectrum needs of the entire HIBS area. With known HIBS area radius, the area of 1 cell can be estimated by one of seven hexagons of equal area, which is:

$$TheareaofHIBScell = \frac{1}{4}\sqrt{3} \cdot HIBSRadius^2 \qquad (21)$$

The capacity demand estimates of Band1, Band2 and Band3 for HIBS Downlink in 2010, 2015 and 2020 are calculated by result of Table 7 and (21), as well as illustrated in Table 8. It is worth noting that the data in the Table 8 for 2025 is calculated by polynomial fitting as a prediction of capacity demand in 2025.

As for the uplink traffic prediction of HIBS in 2025, according to the actual network usage in China, it is estimated according to 1/8 of the downlink traffic. The capacity demand of uplink is shown in Table 9.

TABLE 9. Capacity demand of HIBS uplink.

Uplink	Band1	Band2	Band3
2025 Traffic Prediction/cell (Mbps)	5.91	5.91	4.78

TABLE 10. Spectrum needs prediction of 2025.

	Band1	Band2	Band3
Downlink Spectral Efficiency (bps/Hz)	1.09	0.74	0.65
Uplink Spectral Efficiency (bps/Hz)	0.16	0.1	0.08
2025 Downlink Capacity Prediction/cell (Mbps)	47.27	47.27	38.27
2025 Uplink Capacity Prediction/cell (Mbps)	5.91	5.91	4.78
2025 Downlink Spectrum Prediction (MHz)	43.37	63.88	58.88
2025 Uplink Spectrum Prediction (MHz)	36.93	59.09	59.80
2025 Total Spectrum Prediction (MHz)	80.30	122.97	118.67

On the basis of the simulation results of the spectral efficiency in Table 3 and the capacity demand prediction above, the prediction results of spectrum needs in 2025 was calculated by *CapacityDemand*/*SpectralEfficiency*, which is illustrated in Table 10.

Based on the above prediction process, the total spectrum needs of HIBS in 2025 range from 80.30 MHz to 122.97 MHz. The spectrum needs will change depending on the frequency band and the spectral efficiency. It should be noted that HIBS is deployed independently in our prediction scenario, so interference from other systems is not taken into account. Interference from other systems can cause the higher HIBS spectrum needs than the predicted HIBS spectrum needs.

V. CONCLUSION

Through system simulation and traffic prediction, this paper shows that the spectrum needs range of HIBS as a supplement to IMT network in remote areas in 2025 is 80.30 MHz to 122.97 MHz. What this paper provides is only an evaluation method of spectrum needs, a stand-alone balloon providing Internet access to a remote area is a limited example of what is possible, In the future, more application scenarios of HAPS may be actually deployed, requiring more spectrum

and higher frequency bands, which can be evaluated using the method in this paper.

REFERENCES

[1] *Study on New Radio (NR) to Support Non-Terrestrial Networks V.15.4.0 (Rel. 15)*, Sophia Antipolis, France, document 3GPP 38.811, 2020.

[2] M. S. Alam, G. K. Kurt, H. Yanikomeroglu, P. Zhu, and N. D. Dao, "High altitude platform station based super macro base station constellations," *IEEE Commun. Mag.*, vol. 59, no. 1, pp. 103–109, Jan. 2021.

[3] K. Hoshino, S. Sudo, and Y. Ohta, "A study on antenna beamforming method considering movement of solar plane in HAPS system," in *Proc. IEEE 90th Veh. Technol. Conf. (VTC-Fall)*, Sep. 2019, pp. 1–5.

[4] ITU. (2016). *Radio Regulations Articles*. [Online]. Available: http://www.itu.int/pub/R-REG-RR-2016

[5] T. C. Tozer and D. Grace, "High-altitude platforms for wireless communications," *Electron. Commun. Eng. J.*, vol. 13, no. 3, pp. 127–137, Jun. 2001.

[6] X.-Z. Gao, Z.-X. Hou, Z. Guo, J.-X. Liu, and X.-Q. Chen, "Energy management strategy for solar-powered high-altitude long-endurance aircraft," *Energy Convers. Manage.*, vol. 70, pp. 20–30, Jun. 2013.

[7] A. Alsahlani, L. J. Johnston, and P. A. Atcliffe, "Design of a high altitude long endurance flying-wing solar-powered unmanned air vehicle," *Prog. Flight Phys.*, vol. 9, pp. 3–24, Oct. 2017.

[8] J. Qiu, D. Grace, G. Ding, M. D. Zakaria, and Q. Wu, "Air-ground heterogeneous networks for 5G and beyond via integrating high and low altitude platforms," *IEEE Wireless Commun.*, vol. 26, no. 6, pp. 140–148, Dec. 2019.

[9] J. Gavan, S. Tapuchi, and D. Grace, "Concepts and main applications of high-altitude-platform radio relays," *URSI Radio Sci. Bull.*, vol. 2009, no. 330, pp. 20–31, Sep. 2009.

[10] A. K. Widiawan and R. Tafazolli, "High altitude platform station (HAPS): A review of new infrastructure development for future wireless communications," *Wireless Pers. Commun.*, vol. 42, no. 3, pp. 387–404, Jun. 2007.

[11] J. Thornton, D. Grace, C. Spillard, T. Konefal, and T. Tozer, "Broadband communications from a high-altitude platform: The European HeliNet programme," *Electron. Commun. Eng. J.*, vol. 13, no. 3, pp. 138–144, Jun. 2001.

[12] A. Aragon-Zavala, J. L. Cuevas-Ruíz, and J. A. Delgado-Penín, *High Altitude Platforms for Wireless Communications*. Hoboken, NJ, USA: Wiley, 2008.

[13] D. Grace and M. Mohorcic, *Broadband Communications Via High Altitude Platforms*. Hoboken, NJ, USA: Wiley, 2011.

[14] E. Cianca, R. Prasad, M. De Sanctis, A. De Luise M. Antonini, D. Teotino, and M. Ruggieri, "Integrated satellite-HAP systems," *IEEE Commun. Mag.*, vol. 43, no. 12, pp. 33–39, Dec. 2005.

[15] P. D. Arapoglou, E. T. Michailidis, A. D. Panagopoulos, A. G. Kanatas, and R. Prieto-Cerdeira, "The land mobile Earth-space channel," *IEEE Veh. Technol. Mag.*, vol. 6, no. 2, pp. 44–53, Jun. 2011.

[16] A. G. Kanatas and A. D. Panagopoulos, *Radio Wave Propagation and Channel Modeling for Earth-Space Systems*. Boca Raton, FL, USA: CRC Press, 2016.

[17] Z. Hasirci, "Propagation modeling and performance analysis on the high-altitude platform stations (HAPs)," M.S. dissertation, Dept. Elect. Electron. Eng., Karadeniz Technical Univ., Trabzon, Turkey, 2011.

[18] Z. Hasirci and I. H. Cavdar, "Propagation modeling dependent on frequency and distance for mobile communications via high altitude platforms (HAPs)," in *Proc. 35th Int. Conf. Telecommun. Signal Process. (TSP)*, Jul. 2012, pp. 287–291.

[19] G. Karabulut Kurt, M. G. Khoshkholgh, S. Alfattani, A. Ibrahim, T. S. J. Darwish, M. Sahabul Alam, H. Yanikomeroglu, and A. Yongacoglu, "A vision and framework for the high altitude platform station (HAPS) networks of the future," *IEEE Commun. Surveys Tuts.*, vol. 23, no. 2, pp. 729–779, 2nd Quart., 2021.

[20] S. C. Arum, D. Grace, and P. D. Mitchell, "A review of wireless communication using high-altitude platforms for extended coverage and capacity," *Comput. Commun.*, vol. 157, no. 1, pp. 232–256, May 2020.

[21] D. Yuniarti, "Regulatory challenges of broadband communication services from high altitude platforms (HAPs)," in *Proc. Int. Conf. Inf. Commun. Technol. (ICOIACT)*, Mar. 2018, pp. 919–922.

[22] H. Liu and F. Tronchetti, "Regulating near-space activities: Using the precedent of the exclusive economic zone as a model?" *Ocean Develop. Int. Law*, vol. 50, nos. 2–3, pp. 91–116, Feb. 2019.

[23] *Sharing and Compatibility Studies of HAPS Systems in the Fixed Service in the 21.4–22 GHz Frequency Range for Region 2*, ITU, Geneva, Switzerland, document F.2471-0, 2019.

[24] *Sharing and Compatibility Studies of HAPS Systems in the Fixed Service in the 24.25–27.5 GHz Frequency Range in Region 2*, ITU, Geneva, Switzerland, document F.2472-0, 2019.

[25] *Sharing and Compatibility Studies of High-Altitude Platform Station Systems in the Fixed Service in the 38–39.5 GHz Frequency Range*, ITU, Geneva, Switzerland, document F.2475-0, 2019.

[26] *World Radio Communication Conference 2019 (WRC-19) Final Acts: Resolution 247*, ITU, Geneva, Switzerland, 2019.

[27] *Recommendation ITU-R M.2101, Modelling and Simulation of IMT Networks and Systems for Use in Sharing and Compatibility Studies*, document ITU.2017.08, 2017.

[28] *Recommendation ITU-R P.525-4, Calculation of Free-Space Attenuation*, document ITU.2019.08, 2019.

[29] *Report ITU-R M.2290-0, Future Spectrum Requirements Estimate for Terrestrial IMT*, document ITU.2013.12, 2013.

[30] *Recommendation ITU-R M.1768-1, Methodology for Calculation of Spectrum Requirements for the Terrestrial Component of International Mobile Telecommunications*, document ITU.2013.04, 2013.

[31] *The Spectrum Requirement Estimation Tool for IMT*. ITU-R., 2013. [Online]. Available: https://www.itu.int/dms_pub/itu-r/oth/0a/06/R0A060000580002XLSE.xls

YUETIAN ZHOU received the B.S. and master's degrees in communication engineering from the Beijing University of Posts and Telecommunications, Beijing, China, in 2015 and 2018, respectively. He is currently pursuing the Ph.D. degree in electronic information major with the National Key Laboratory of Science and Technology on Communication, University of Electronic Science and Technology of China. He is also a Junior Researcher at the Mobile Communication Department, China Telecom Research Institute. In recent years, his work focuses on 4G/5G spectrum sharing, spectrum compatibility and sharing, HAPS, and full duplex.

FEI QI received the master's degree in information and communication engineering from the Beijing University of Posts and Telecommunications, in 2015, and the Ph.D. degree, in 2022. He is currently working as an Engineer at China Telecom. He is active in standards development, such as ITU-R WP 5D and CCSA. He has published many academic papers and patents. He is responsible for spectrum simulation projects as the Project Leader. His research interests include the Internet of Things, vehicular networks, massive MIMO precoding, artificial intelligence, and channel estimation.

WEILIANG XIE received the B.E. and M.E. degrees in information science and technology from Nankai University, Tianjin, China, in 1997 and 2000, respectively, and the Ph.D. degree in information science and technology from Peking University, Beijing, China, in 2003. He is currently a Senior Engineer (Professor-level) with China Telecom Corporation Ltd., Technology Innovation Center, Beijing. His research interests include mobile networks, wireless communication systems, and air to ground communications.